

Electronic Supporting Information for:
Covalently integrated silica nanoparticles in poly(ethylene glycol)-
based acrylate resins: thermomechanical, swelling, and
morphological behavior

Alexis Hocken¹, Frederick L. Beyer², Jae Sang Lee¹, Bradley J. Grim¹, Husain Mithaiwala¹, and
Matthew D. Green^{1,*}

¹Department of Chemical Engineering; School for Engineering of Matter, Transport and Energy, Arizona State University, Tempe, AZ 85287, USA

²U.S. DEVCOM Army Research Laboratory, Aberdeen Proving Ground, MD 21005, USA

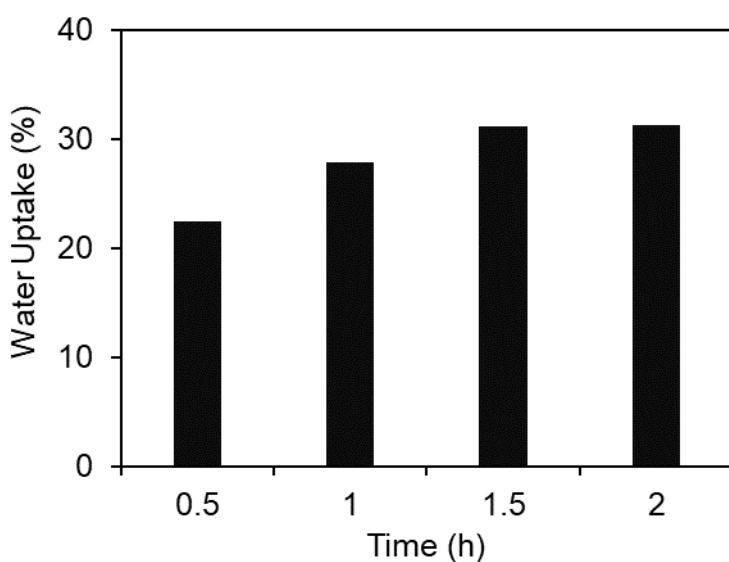


Figure S1. Equilibrium experiments using a composite sample with 16 wt% bare SiO₂ nanoparticles to determine the appropriate time period for water uptake experiments.

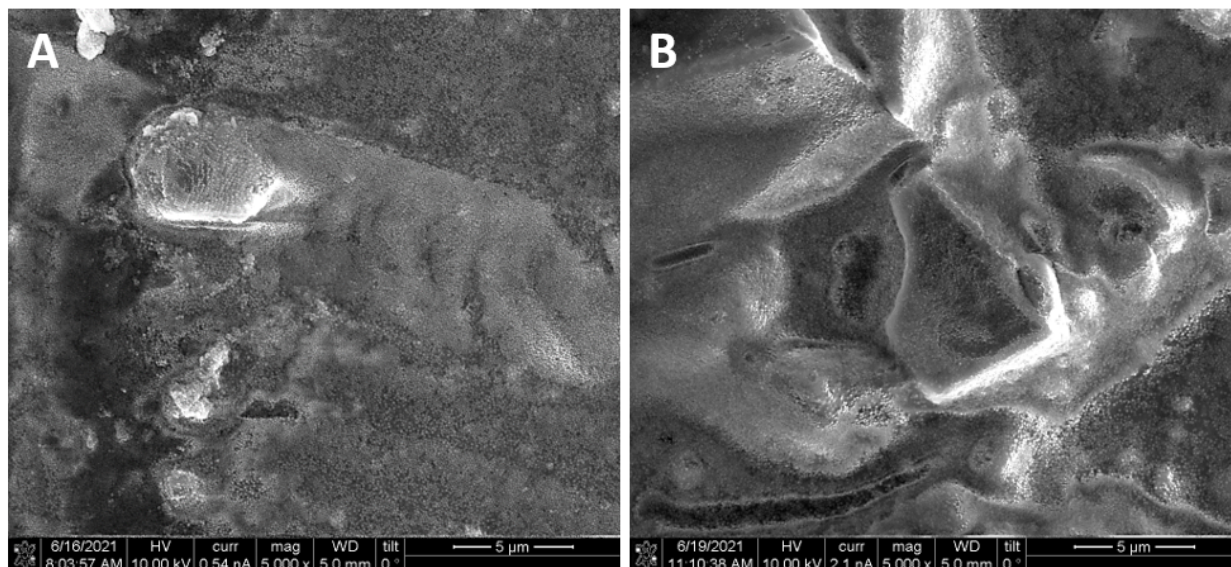


Figure S2. SEM images of the surface of the A) 13.8 wt% MA-SiO₂ and B) 13.8 wt% V-SiO₂.

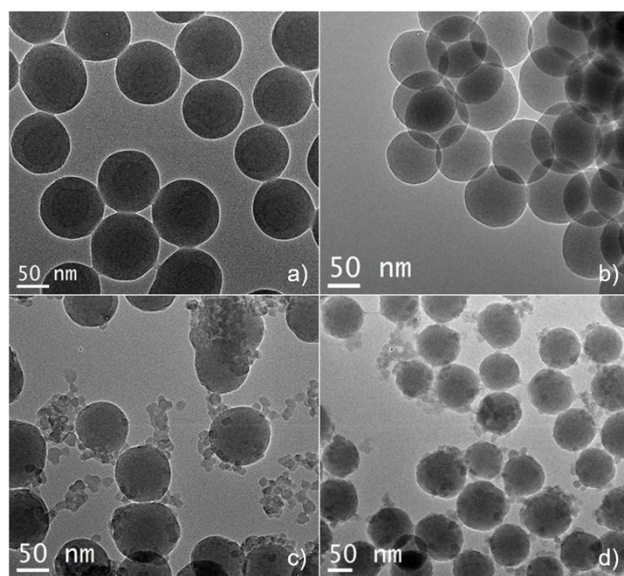


Figure S3. TEM images of MA-SiO₂ nanoparticles dispersed in a) methanol and b) THF. V-SiO₂ nanoparticles dispersed in c) methanol and d) THF.

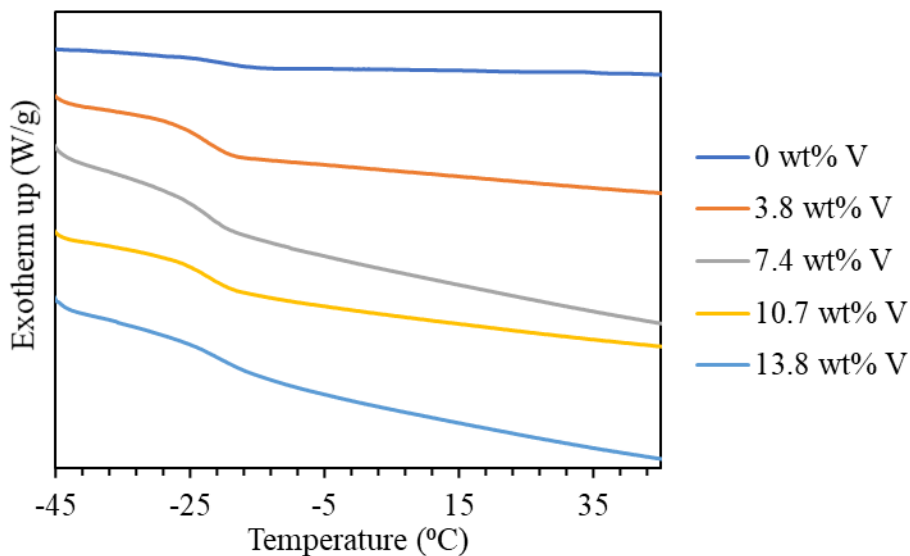


Figure S4. Differential scanning calorimetry (DSC) thermograms of V-SiO₂-loaded nanocomposites. The curves have been shifted vertically for clarity. The glass transition temperature (T_g) was determined using the T_g function in the TRIOS software.

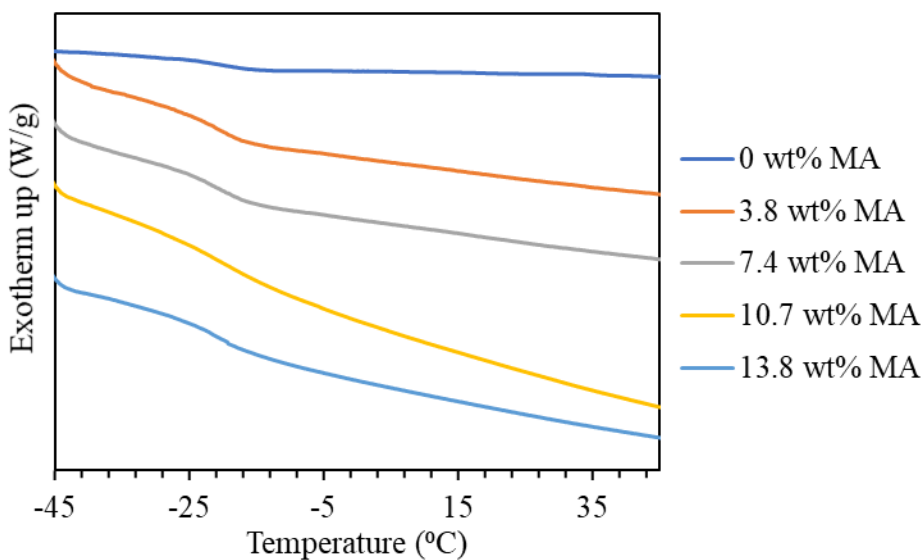


Figure S5. Differential scanning calorimetry (DSC) thermograms of V-SiO₂-loaded nanocomposites. The curves have been shifted vertically for clarity. The glass transition temperature (T_g) was determined using the T_g function in the TRIOS software.

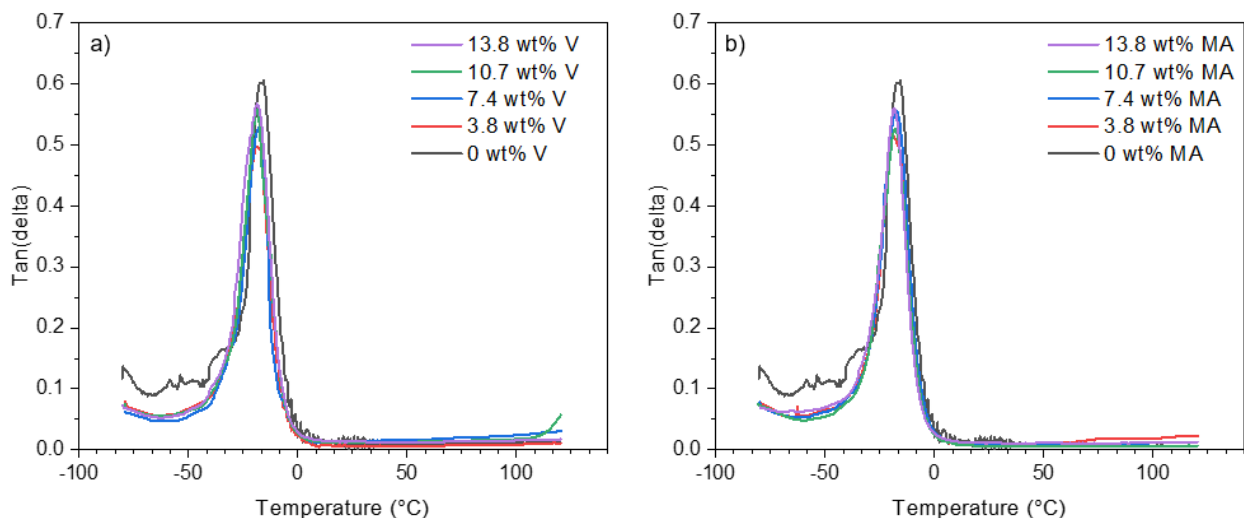


Figure S6. $\text{Tan}(\delta)$ curves as a function of temperature for composite series containing (a) V-SiO₂ nanoparticles and (b) MA-SiO₂ nanoparticles. The maximum of each curve was used to determine the T_g measured by DMA.

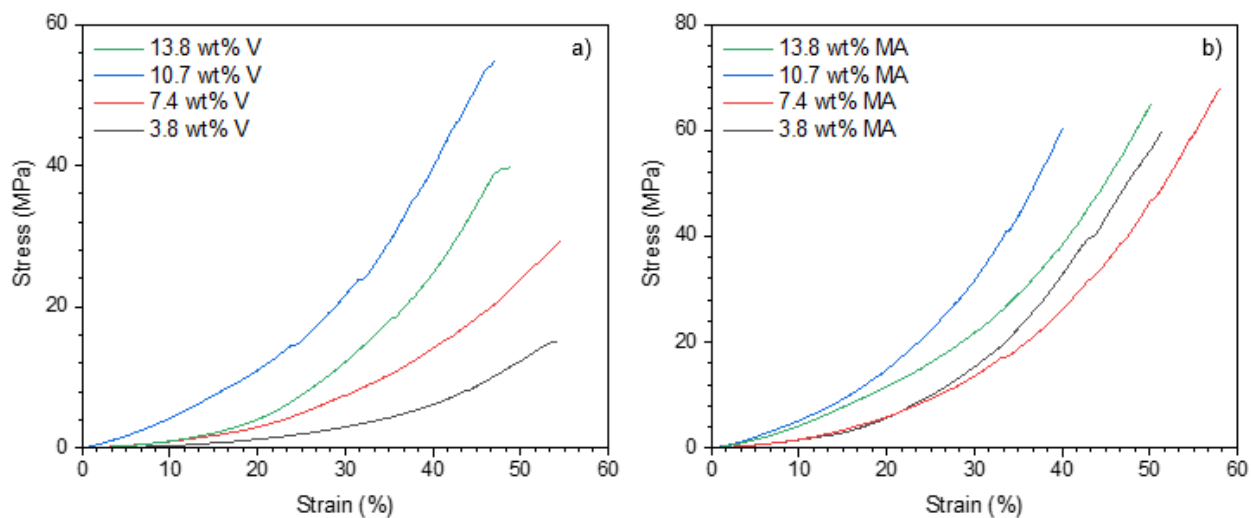


Figure S7. Representative stress vs. strain curves for composite series containing (a) V-SiO₂ nanoparticles and (b) MA-SiO₂ nanoparticles. Small, jagged steps represent the sample chipping slightly due to slight non-uniformity in sample thickness.

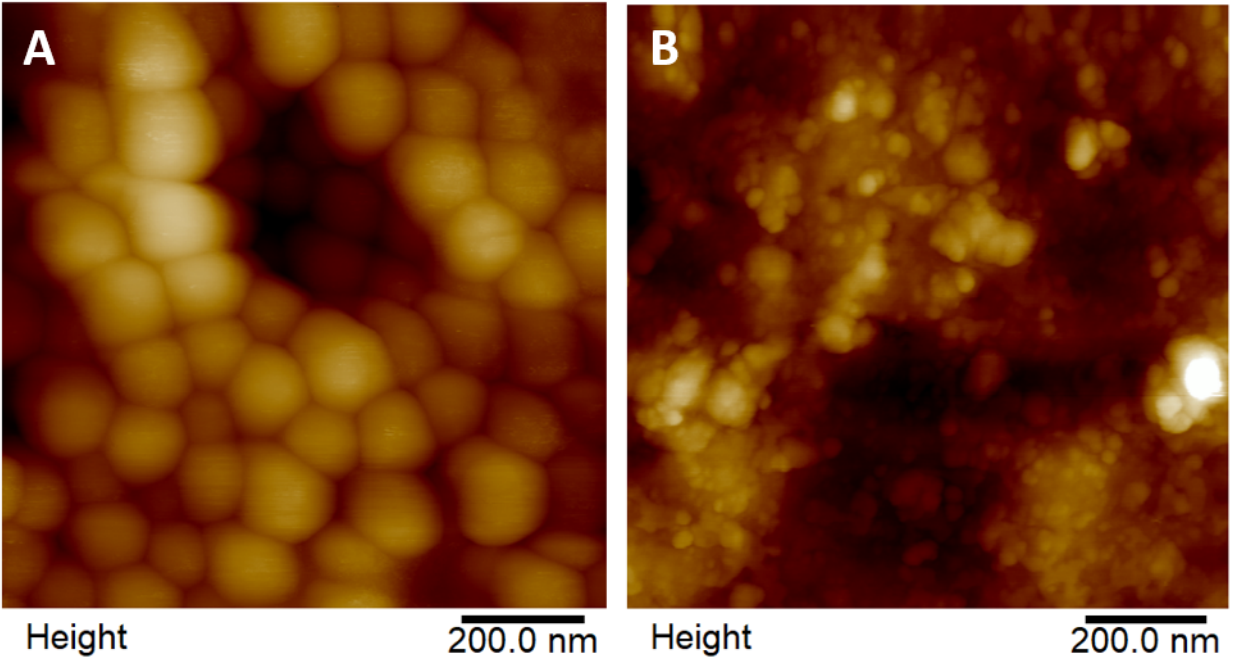


Figure S8. AFM micrographs of aggregates in A) 13.8 wt% MA-SiO₂ and B) 13.8 wt% V-SiO₂, illustrating the effect of the presence of small (12 nm diameter) nanoparticles on the surface structure of the aggregates.

Additional information regarding SAXS data analysis

Analysis of the SAXS data was performed using the modeling tools included in the “Irena” package of macros for use in Igor Pro (Wavemetrics, Inc.), provided by Argonne National Laboratory.¹ The scattering length densities, ρ , of silica (nanoparticles) and the poly(ethylene oxide) (PEO, matrix) were calculated to be $1.04 \times 10^{11} \text{ cm}^{-2}$ and $2.23 \times 10^{11} \text{ cm}^{-2}$, respectively, leading to a very strong scattering contrast, $(\Delta\rho)^2$, of $1.40 \times 10^{22} \text{ cm}^{-4}$.

The following table summarizes the key parameters of the size distributions, including mean particle radius and particle radius distribution width (standard deviation, σ). Fraction is a scaling parameter that is inversely related to scattering contrast. When a structure factor was used, the structure factor radius is given. For one sample (13.8 wt% V-SiO₂), a third particle population was added to account explicitly for scattering from large particles that remained dilute.

Table S1. Fitting parameters used to generate model scattering functions to fit the SAXS data.

Sample	Large Particles				Small Particles				Large Particles (dilute)		
	Radius (Å)	Radius σ (Å)	Fraction	SF Radius (Å)	Radius (Å)	Radius σ (Å)	Fraction	SF Radius (Å)	Radius (Å)	Radius σ (Å)	Fraction
3.8 wt% MA-SiO ₂	532	27	0.0038	N/A	-	-	-	-	-	-	-
7.4 wt% MA-SiO ₂	532	27	0.0071	672	-	-	-	-	-	-	-
10.7 wt% MA-SiO ₂	532	27	0.0037	630	-	-	-	-	-	-	-
13.8 wt% MA-SiO ₂	532	27	0.016	698	-	-	-	-	-	-	-
3.8 wt% V-SiO ₂	460	37	0.0024	464	54	7.9	0.00041	-	-	-	-
7.4 wt% V-SiO ₂	460	37	0.0034	464	59	14	0.00093	-	-	-	-
10.7 wt% V-SiO ₂	460	37	0.0072	464	55	8.6	0.0014	-	-	-	-
13.8 wt% V-SiO ₂	460	37	0.0042	471	65.8	44.3	0.0022	73.6	460	37	0.0025

In general terms, the data were fit using the form factor for a spherical particle in either the dilute limit or with interparticle interference modeled using the Percus-Yevick hard sphere structure factor. The V-SiO₂ samples were found to have scattering at higher angles from much smaller particles, necessitating the addition of a second size distribution. The form factor for a spherical particle was used for this second size distribution as well. For all form factors, a Gaussian distribution of particle sizes (radii) was assumed for simplicity.

Once a “good” value was determined for the radius and width of the size distribution for the large nanoparticles, that value was used in all the fits for samples filled from that specific lot of silica nanoparticles. However, for the particle fraction having the smaller size, the radius and width values were allowed to vary on the assumption that the smaller particle fraction was an

impurity, not included in the starting materials intentionally, and thus not subject to the same synthetic controls as the larger particles.

The general fitting procedure, particularly for the samples containing V-SiO₂ nanoparticles, involved many steps and iterations with manual adjustments of fitting parameters. Once an approximate fit was obtained, final fitting was then performed working from low- q to high- q , fitting one set of features at a time. In the region where overlap occurred between scattering from large and small nanoparticles, multiple contributing features sometimes were fit simultaneously. The preferred final fit would involve fitting all parameters simultaneously, but was not always feasible for samples where the fit was marginal.

1. Ilavsky, J.; Jemian, P. R. *J. Appl. Crystallogr.* **2009**, *42*, 347-353.